Electronic Supplementary Material (ESI) for Chemical Science


# Supporting Information

## Chemical transformations of a crystalline coordination polymer: a multi-stage solid-vapour reaction manifold

Iñigo J. Vitórica-Yrezábal,[1] Guillermo Mínguez Espallargas,[2] Janet Soleimannejad,[3] Alastair J. Florence,[4] Ashleigh J. Fletcher,[5] Lee Brammer*,[1]

*Email: lee.brammer@sheffield.ac.uk*

[1] *Department of Chemistry, University of Sheffield, Sheffield S3 7HF, UK.*
[2] *Instituto de Ciencia Molecular (ICMol), Universidad de Valencia, c/ Catedrático José Beltrán, 2, 46980 Paterna, Spain.*
[3] *School of Chemistry, College of Science, University of Tehran, Tehran, Iran*
[4] *Strathclyde Institute of Pharmacy and Biomedical Sciences, University of Strathclyde, 27 Taylor Street, Glasgow G4 0NR, Scotland.*
[5] *Department of Chemical and Process Engineering, University of Strathclyde, 75 Montrose St, Glasgow G1 1XJ, Scotland.*

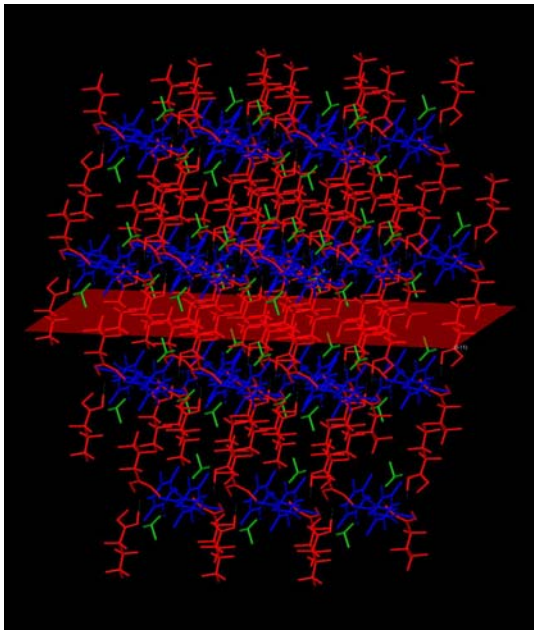

**Figure S1.** Hexagonal rod packing of coordination polymers in the crystal structure of **1-MeOH** viewed perpendicular to plane (−101), with plane (01−1) containing the fluorous layer shown in red. (TMP ligands are shown in blue, heptafluorobutanoate in red and methanol in green).

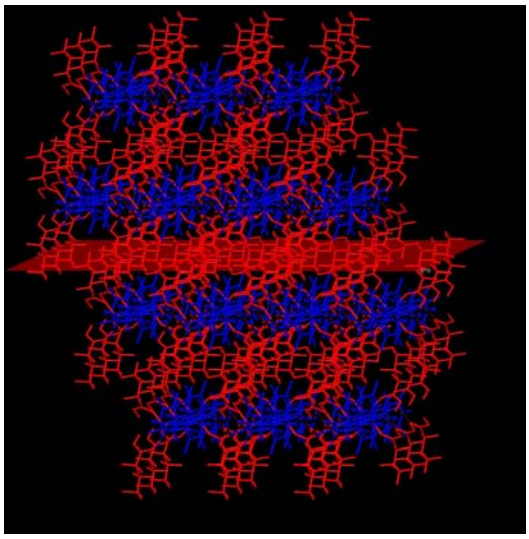

**Figure S2.** Hexagonal rod packing of coordination polymers in the crystal structure of **1** viewed perpendicular to plane (100), with plane (010) containing the fluorous layer shown in red. Colours as in Figure S1.

**Phase purity of 1-MeOH.** A polycrystalline sample of **1-MeOH** was lightly ground in an agate mortar and pestle and loaded into a 0.7 mm borosilicate glass capillary prior to being mounted and aligned on a Bruker-AXS D8 Advance powder diffractometer operating with Ge-monochromated Cu $K_{\alpha 1}$ radiation ($\lambda$ = 1.54056 Å). The powder pattern was measured at a scan rate of 1 °/min in the range $4 \leq 2\theta \leq 40$ °. A unit cell was found corresponding to crystal structure of **1-MeOH** already established from single crystal diffraction. Pawley refinement[S1] was performed for the full pattern using the program TOPAS.[S2] Refinement converged to $R_{wp}$ = 0.0514, $R_{wp}'$ = 0.1324 ($R_{wp}$' is the background subtracted $R_{wp}$); see Figure S5.

**Phase purity of 1-EtOH.** White microcrystalline **1-EtOH**, product of the solution phase synthesis, was loaded into a 0.7mm borosilicate capillary and X-ray diffraction data were collected ($\lambda$= 0.799993(8) Å) at station ID31[S3] at the European Synchrotron Radiation Source (ESRF) using a 9-channel multi-analyser crystal (MAC) detector. All data were collected at room temperature. The powder pattern was indexed using the program TOPAS.[S2] A unit cell was found corresponding to crystal structure of **1-EtOH** already established from single crystal diffraction. The starting model used for Rietveld refinement,[S4] conducted using TOPAS, was the single crystal structure of **1-EtOH.** The model for the structure was refined with one global isotropic thermal parameter. A 6$^{th}$ order spherical harmonic correction of the intensities for preferred orientation was applied in the final stage of refinement.

Rietveld refinement converged to $R_{wp}$ of 0. 14630 , $R_{wp}$' = 0.23936 ($R_{wp}$' is the background subtracted $R_{wp}$); see Figure S3.

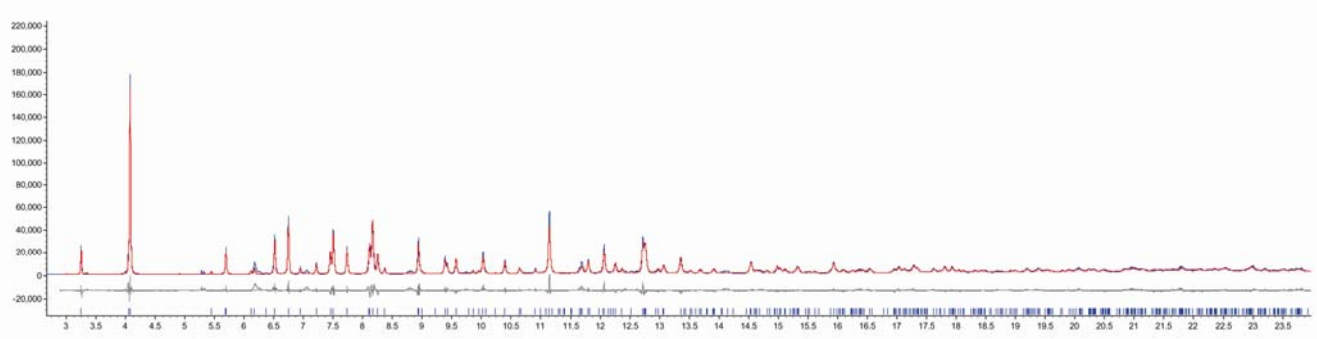

**Figure S3** Observed (blue) and calculated (red) profiles and difference plot [$I_{obs}$-$I_{calc}$] (grey) of the Rietvield refinement. (2θ range: 3.0 – 24°; maximum resolution 1.9238Å).

**Phase purity of 1-$^{i}$PrOH.** White microcrystalline **1-$^{i}$PrOH**, product of the solid-vapour synthesis from **1** and $^{i}$PrOH, was loaded into a 0.7mm borosilicate capillary and X-ray diffraction data were collected (λ= 0.826741(1) Å) at beamline I11 at Diamond Light Source,[S5] equipped with a wide angle (90 °) PSD detector comprising multiple Mythen-2 modules. A series of 14 pairs of scans were conducted at room temperature, each pair related by a 0.25 ° detector offset to account for gaps between detector modules. The resulting 28 patterns were summed to give the final pattern for structural analysis. The powder pattern was indexed using the program TOPAS.[S2] A unit cell was found corresponding to the known crystal structure of **1-$^{i}$PrOH**. The starting model used for Rietveld refinement,[S4] conducted using TOPAS, was the single crystal structure of **1-$^{i}$PrOH.** This model was refined with one global isotropic thermal parameter. A 6$^{th}$ order spherical harmonic correction of the intensities for preferred orientation was applied in the final stage of refinement. Rietveld refinement converged to $R_{wp}$ of 0.10456 , $R_{wp}$' = 0.18195 ($R_{wp}$' is the background subtracted $R_{wp}$); see Figure S4.

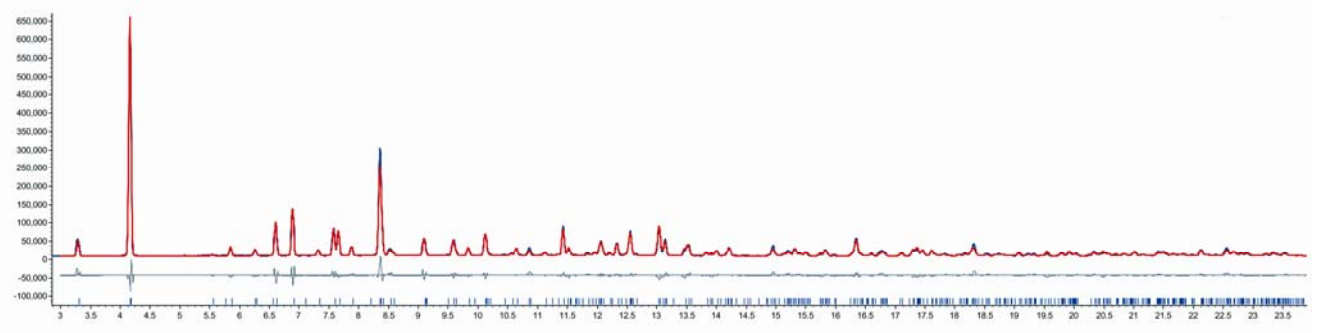

**Figure S4** Observed (blue) and calculated (red) profiles and difference plot [$I_{obs}$-$I_{calc}$] (grey) of the Rietvield refinement. (2θ range: 3.0 – 24°; maximum resolution 1.9882 Å).

**Table S1.** Final $R_{wp}$, $R_{wp'}$ and GOF values for the Pawley refinements to all patterns of the *in situ* study of the reaction sequence **1-MeOH→(1+1$^{HT}$)→2**

| | *T (K)* | $R_{wp}$ | $R_{wp'}$ | GOF | phases included in fit |
|---|---|---|---|---|---|
| Pattern 1 (Fig. S5) | 300 | 0.0518 | 0.1334 | 1.488 | **1-MeOH** |
| Pattern 2 (Fig. S6) | 320 | 0.0579 | 0.1034 | 1.851 | **1-MeOH, 1, 1$^{HT}$** |
| Pattern 3 (Fig. S7) | 320 | 0.0478 | 0.0848 | 1.531 | **1-MeOH, 1, 1$^{HT}$** |
| Pattern 4 (Fig. S8) | 380 | 0.0465 | 0.1000 | 1.443 | **1, 1$^{HT}$** |
| Pattern 5 (Fig. S9) | 390 | 0.0461 | 0.0871 | 1.428 | **1, 1$^{HT}$** |
| Pattern 6 (Fig. S10) | 400 | 0.0450 | 0.0786 | 1.390 | **1, 1$^{HT}$, 2** |
| Pattern 7 (Fig. S11) | 400 | 0.0483 | 0.0897 | 1.491 | **1, 1$^{HT}$, 2** |
| Pattern 8 (Fig. S12) | 420 | 0.0518 | 0.1006 | 1.609 | **1, 1$^{HT}$, 2** |
| Pattern 9 (Fig. S13) | 420 | 0.0459 | 0.0874 | 1.425 | **1, 1$^{HT}$, 2** |
| Pattern 10 (Fig. S14) | 420 | 0.0469 | 0.0907 | 1.460 | **1, 1$^{HT}$, 2** |
| Pattern 11 (Fig. S15) | 420 | 0.0454 | 0.0892 | 1.411 | **1, 1$^{HT}$, 2** |
| Pattern 12 (Fig. S16) | 420 | 0.0453 | 0.0867 | 1.403 | **1, 1$^{HT}$, 2** |
| Pattern 13 (Fig. S17) | 420 | 0.0479 | 0.0920 | 1.484 | **1, 1$^{HT}$, 2** |
| Pattern 14 (Fig. S18) | 420 | 0.0464 | 0.1059 | 1.283 | **1$^{HT}$, 2** |
| Pattern 15 (Fig. S19) | 420 | 0.0450 | 0.1097 | 1.248 | **1$^{HT}$, 2** |
| Pattern 16 (Fig. S20) | 420 | 0.0447 | 0.1041 | 1.235 | **1$^{HT}$, 2** |
| Pattern 17 (Fig. S21) | 420 | 0.0422 | 0.0979 | 1.160 | **1$^{HT}$, 2** |
| Pattern 18 (Fig. S22) | 420 | 0.0480 | 0.1249 | 1.204 | **2** |
| Pattern 19 (Fig. S23) | 240 | 0.0549 | 0.1360 | 1.329 | **2** |

**Table S2.** Unit cell parameters from Pawley refinements for **1-MeOH** (pattern 1; 300K), **1** and **1$^{HT}$** (pattern 4; 380 K) and **2** (pattern 18; 420 K)

| Compound | a (Å) | b (Å) | c (Å) | α ° | β ° | γ ° | Volume (Å$^3$) |
|---|---|---|---|---|---|---|---|
| **1-MeOH** | 8.914(2) | 12.709(4) | 15.423(2) | 110.50(2) | 96.64(2) | 104.33(2) | 1545.9(8) |
| **1** | 8.587(4) | 12.984(4) | 15.008(7) | 112.73(2) | 90.10(2) | 108.69(1) | 1446(1) |
| **1$^{HT}$** | 14.98(02) | 8.598(7) | 22.77 (2) | 90 | 100.22(9) | 90 | 2886(6) |
| **2** | 10.903(4) | 11.018(5) | 12.697(3) | 73.22(4) | 70.02(3) | 62.697(3) | 1260(1) |

**Pattern 1:**

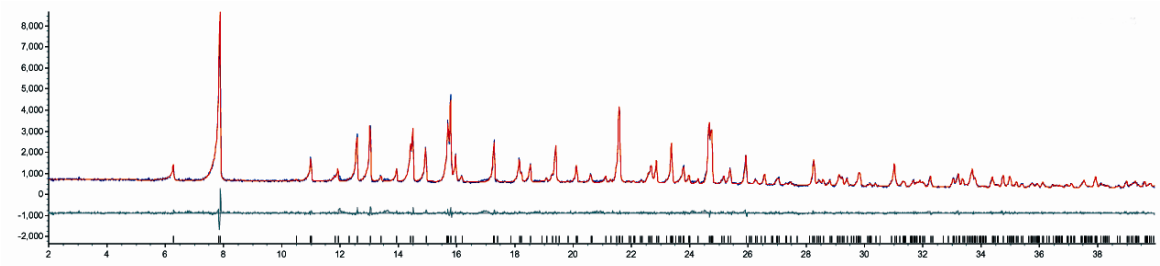


**Figure S5** Observed (blue) and calculated (red) profiles and difference plot [$I_{obs}$-$I_{calc}$] (grey) of the Pawley refinement of Pattern 1 at room temperature (2θ range: 2.0 – 40.0°; maximum resolution 2.25 Å) (only compound **1-MeOH** is present).

**Pattern 2:**

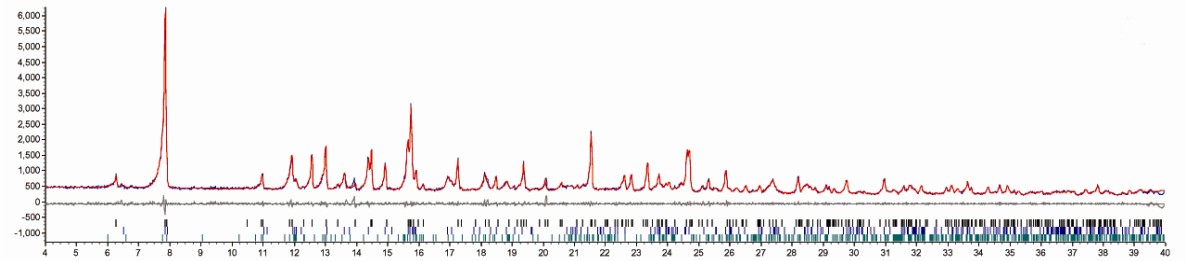

**Figure S6** Observed (blue) and calculated (red) profiles and difference plot [$I_{obs}$-$I_{calc}$] (grey) of the Pawley refinement of Pattern 2 at 320 K (2θ range: 4.0 – 40.0°; maximum resolution 2.25 Å) (compounds **1-MeOH, 1** and **1$^{HT}$** are present).

**Pattern 3:**

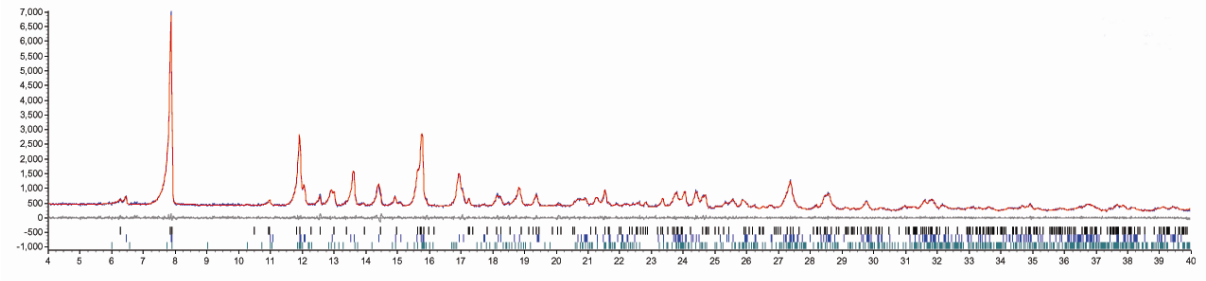

**Figure S7** Observed (blue) and calculated (red) profiles and difference plot [$I_{obs}$-$I_{calc}$] (grey) of the Pawley refinement of Pattern 3 at 320 K (2θ range: 4.0 – 40.0°; maximum resolution 2.25 Å) (compounds **1-MeOH, 1** and **1$^{HT}$** are present).

**Pattern 4:**

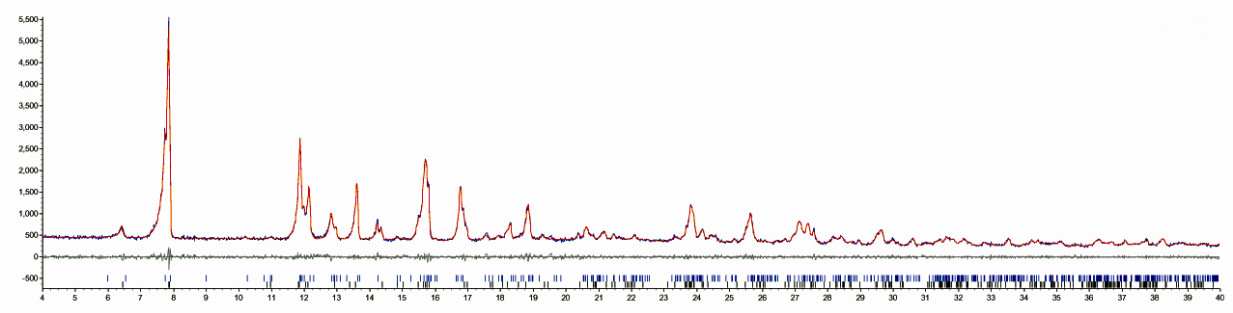

**Figure S8** Observed (blue) and calculated (red) profiles and difference plot [$I_{obs}$-$I_{calc}$] (grey) of the Pawley refinement of Pattern 4 at 380 K (2θ range: 4.0 – 40.0°; maximum resolution 2.25 Å) (compounds **1,** and **1$^{HT}$**).

**Pattern 5:**

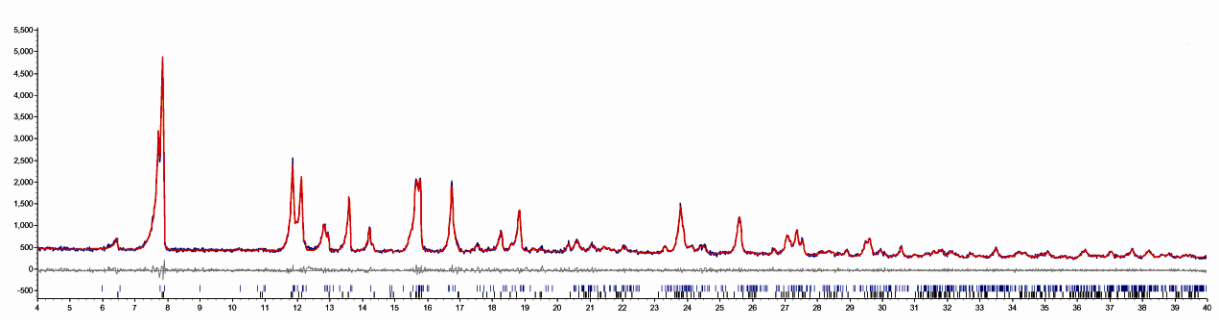

**Figure S9** Observed (blue) and calculated (red) profiles and difference plot [$I_{obs}$-$I_{calc}$] (grey) of the Pawley refinement of Pattern 5 at 390 K (2θ range: 4.0 – 40.0°; maximum resolution 2.25 Å) (compounds **1** and **1$^{HT}$** are present).

**Pattern 6:**

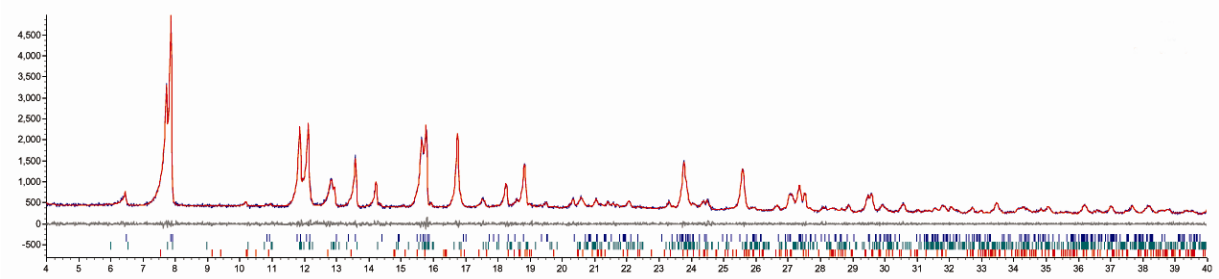

**Figure S10** Observed (blue) and calculated (red) profiles and difference plot [$I_{obs}$-$I_{calc}$] (grey) of the Pawley refinement of Pattern 6 at 400 K (2θ range: 4.0 – 40.0°; maximum resolution 2.25 Å) (compounds **1, 1$^{HT}$** and **2** are present).

**Pattern 7:**

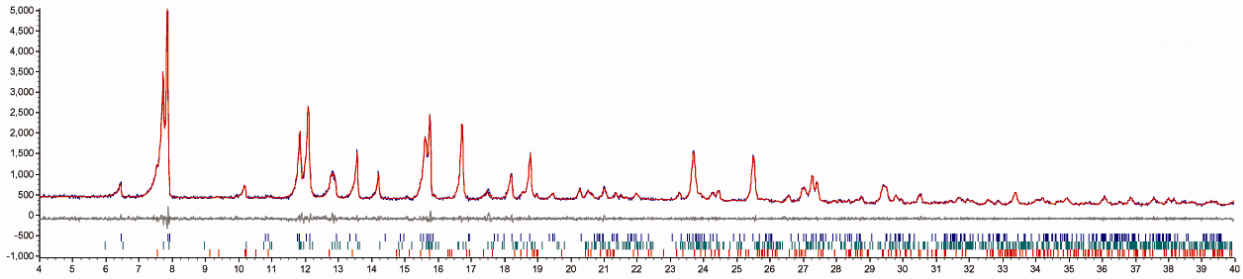

**Figure S11** Observed (blue) and calculated (red) profiles and difference plot [$I_{obs}$-$I_{calc}$] (grey) of the Pawley refinement of Pattern 7 at 400 K (2θ range: 4.0 – 40.0°; maximum resolution 2.25 Å) (compounds **1, 1$^{HT}$** and **2** are present).

**Pattern 8:**

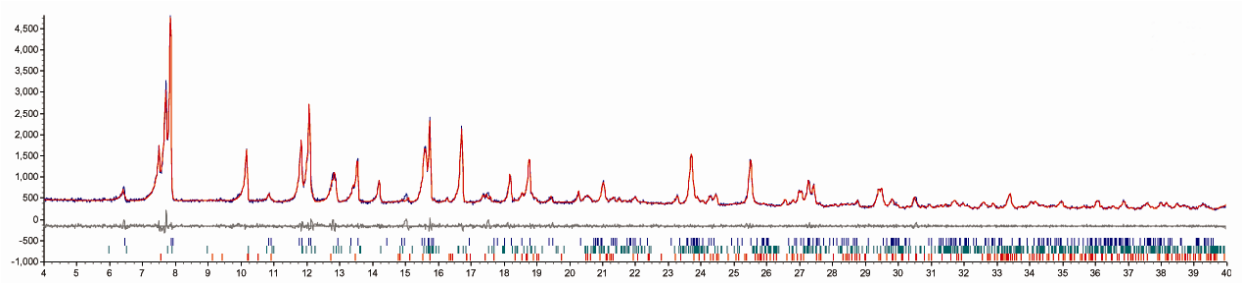

**Figure S12** Observed (blue) and calculated (red) profiles and difference plot [$I_{obs}$-$I_{calc}$] (grey) of the Pawley refinement of Pattern 8 at 420 K (2θ range: 4.0 – 40.0°; maximum resolution 2.25 Å) (compounds **1, 1$^{HT}$** and **2** are present).

**Pattern 9:**

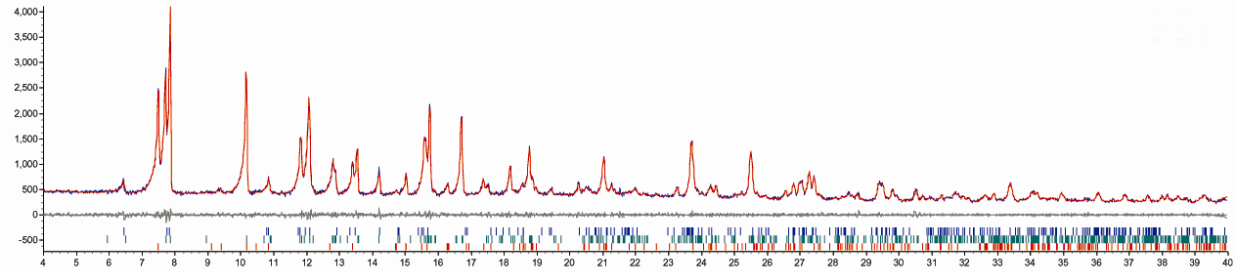

**Figure S13** Observed (blue) and calculated (red) profiles and difference plot [$I_{obs}$-$I_{calc}$] (grey) of the Pawley refinement of Pattern 9 at 420 K (2θ range: 4.0 – 40.0°; maximum resolution 2.25 Å) (compounds **1, 1$^{HT}$** and **2** are present).

**Pattern 10:**

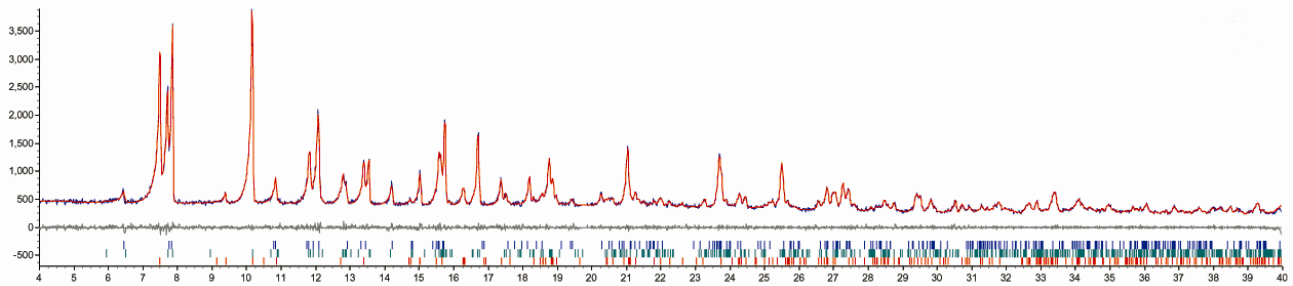

**Figure S14** Observed (blue) and calculated (red) profiles and difference plot [$I_{obs}$-$I_{calc}$] (grey) of the Pawley refinement of Pattern 10 at 420 K (2θ range: 4.0 – 40.0°; maximum resolution 2.25 Å) (compounds **1, 1$^{HT}$** and **2** are present).

**Pattern 11:**

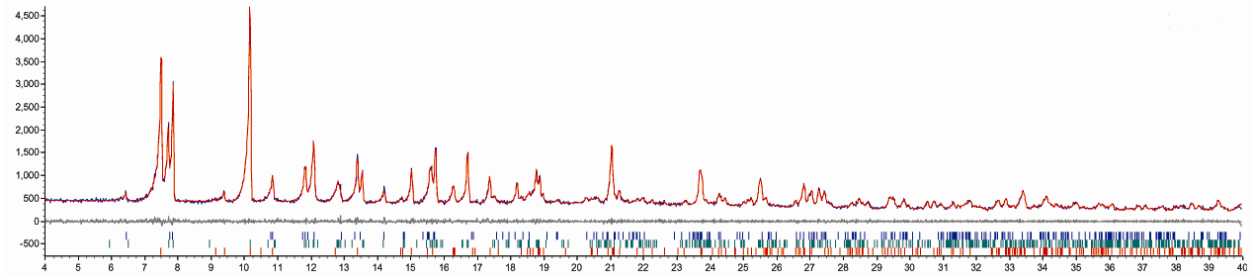

**Figure S15** Observed (blue) and calculated (red) profiles and difference plot [$I_{obs}$-$I_{calc}$] (grey) of the Pawley refinement of Pattern 11 at 420 K (2θ range: 4.0 – 40.0°; maximum resolution 2.25 Å) (compounds **1, 1$^{HT}$** and **2** are present).

**Pattern 12:**

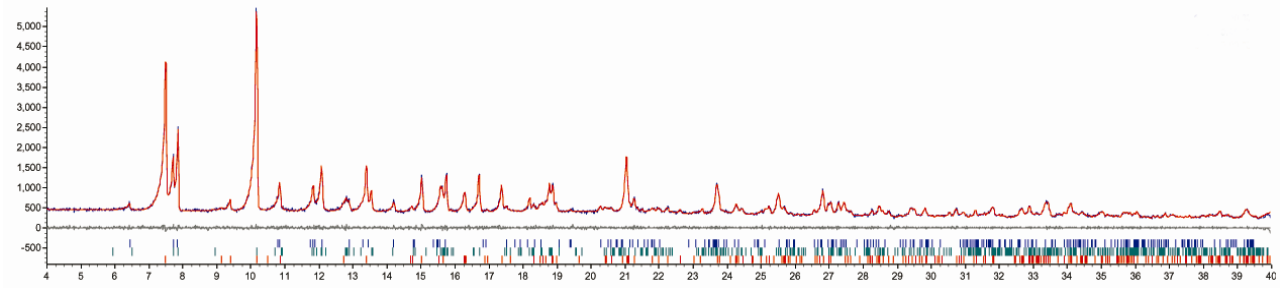

**Figure S16** Observed (blue) and calculated (red) profiles and difference plot [$I_{obs}$-$I_{calc}$] (grey) of the Pawley refinement of Pattern 12 at 420 K (2θ range: 4.0 – 40.0°; maximum resolution 2.25 Å) (compounds **1, 1$^{HT}$** and **2** are present).

**Pattern 13:**

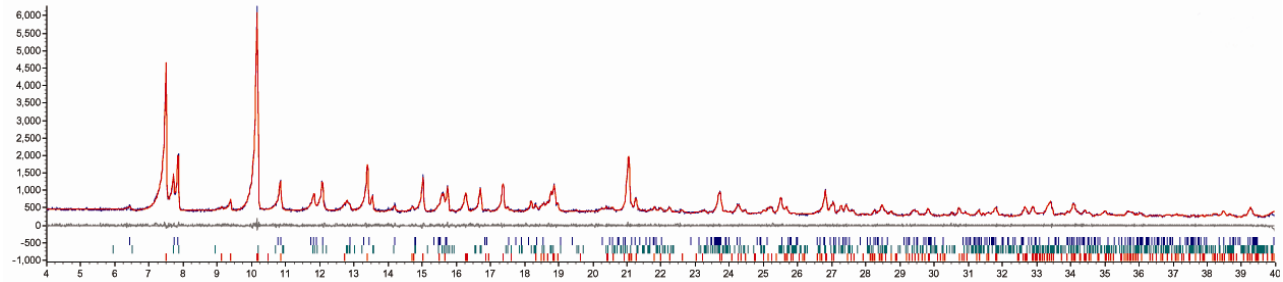

**Figure S17** Observed (blue) and calculated (red) profiles and difference plot [$I_{obs}$-$I_{calc}$] (grey) of the Pawley refinement of Pattern 13 at 420 K (2θ range: 4.0 – 40.0°; maximum resolution 2.25 Å) (compounds **1, 1$^{HT}$** and **2** are present).

**Pattern 14:**

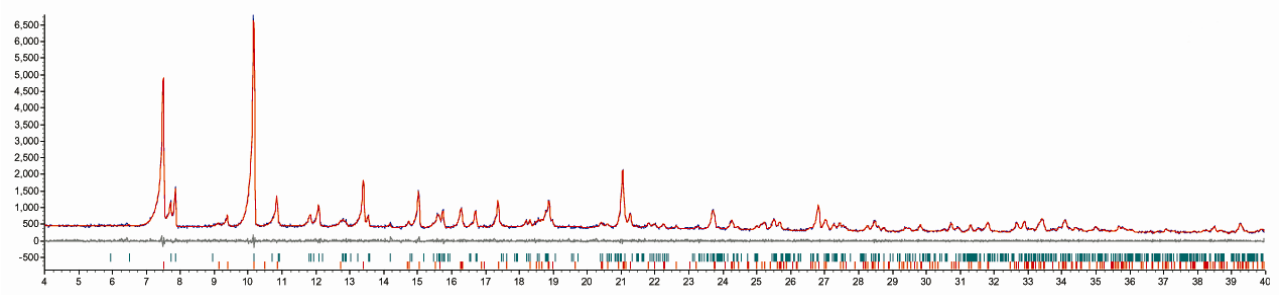

**Figure S18** Observed (blue) and calculated (red) profiles and difference plot [$I_{obs}$-$I_{calc}$] (grey) of the Pawley refinement of Pattern 14 at 420 K (2θ range: 4.0 – 40.0°; maximum resolution 2.25 Å) (compounds **1**$^{HT}$ and **2** are present).

**Pattern 15:**

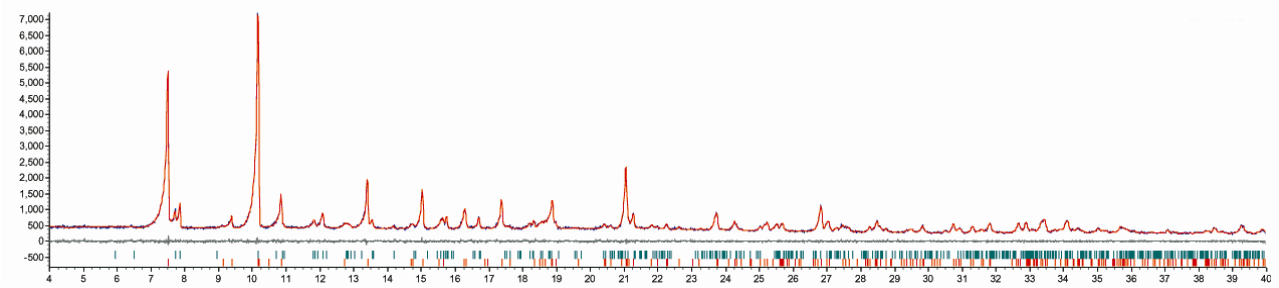

**Figure S19** Observed (blue) and calculated (red) profiles and difference plot [$I_{obs}$-$I_{calc}$] (grey) of the Pawley refinement of Pattern 15 at 420 K (2θ range: 4.0 – 40.0°; maximum resolution 2.25 Å) (compounds **1**$^{HT}$ and **2** are present).

**Pattern 16:**

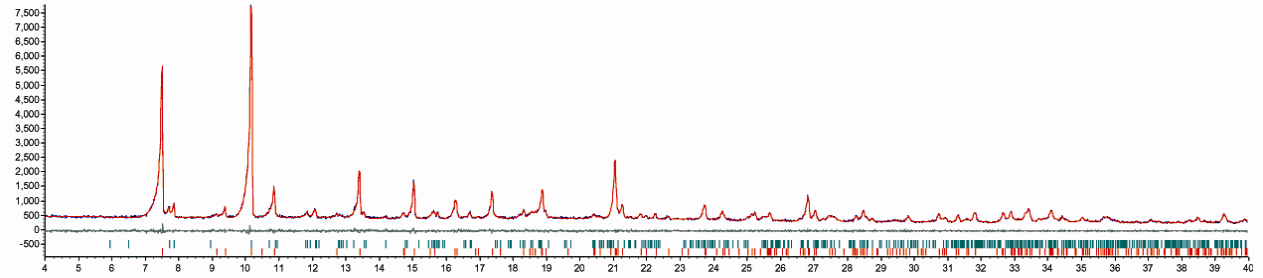

**Figure S20** Observed (blue) and calculated (red) profiles and difference plot [$I_{obs}$-$I_{calc}$] (grey) of the Pawley refinement of Pattern 16 at 420 K (2θ range: 4.0 – 40.0°; maximum resolution 2.25 Å) (compounds **1**$^{HT}$ and **2** are present).

**Pattern 17:**

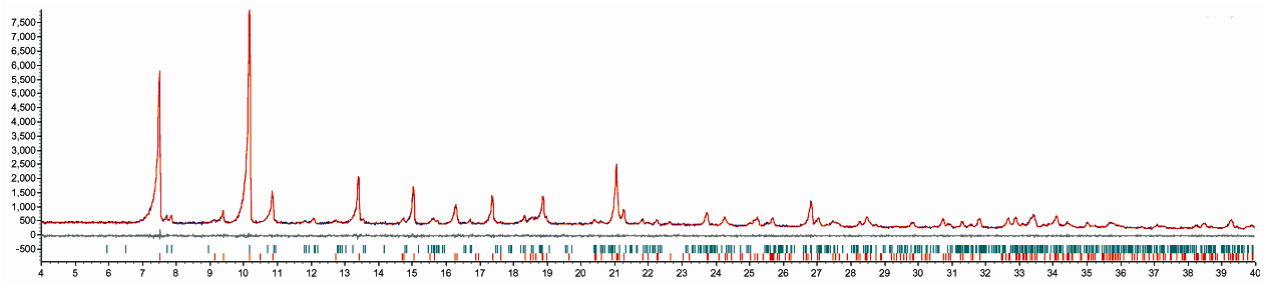

**Figure S21** Observed (blue) and calculated (red) profiles and difference plot [$I_{obs}$-$I_{calc}$] (grey) of the Pawley refinement of Pattern 17 at 420 K (2θ range: 4.0 – 40.0°; maximum resolution 2.25 Å) (compounds **1**$^{HT}$ and **2** are present).

**Pattern 18:**

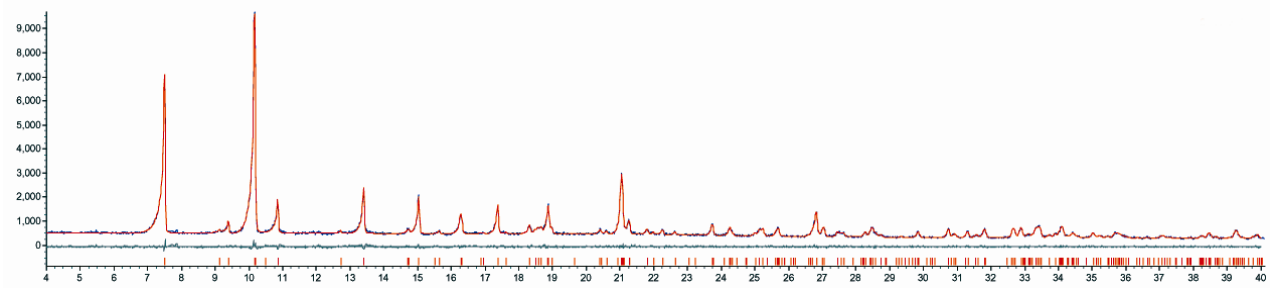

**Figure S22** Observed (blue) and calculated (red) profiles and difference plot [$I_{obs}$-$I_{calc}$] (grey) of the Pawley refinement of Pattern 18 at 420 K (2θ range: 4.0 – 40.0°; maximum resolution 2.25 Å) (only compound **2** is present).

**Pattern 19:**

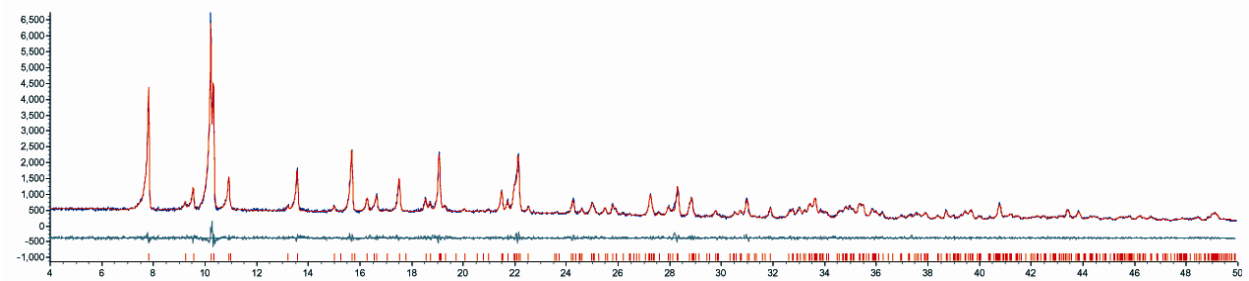

**Figure S23** Observed (blue) and calculated (red) profiles and difference plot [$I_{obs}$-$I_{calc}$] (grey) of the Pawley refinement of Pattern 19 at 240 K (2θ range: 4.0 – 50.0°; maximum resolution 1.82 Å) (only compound **2** is present). Data collected after cooling the sample from 420 to 240 K at the end of the reaction sequence. Pattern is not shown in Figure 4.

**References**

S1. Pawley, G. S. *J. Appl. Cryst.* **1981**, *14*, 357.
S2. Coelho, A. A., *TOPAS-Academic*, version 4.1, 2007; see http://www.topas-academic.net
S3. Fitch, A. N. *J. Res. Natl. Inst. Stand. Technol.* **2004**, *109*, 133.
S4. Rietveld, H. M. *J. Appl. Cryst.* **1969**, *2*, 65.

S5. (a) Thompson, S. P.; Parker, J. E.; Potter, J.; Hill, T. P.; Birt, A.; Cobb, T. M.; Yuan, F.; Tang, C. C. *Rev. Sci. Instrum.* **2009**, *80*, 075107. (b) Thompson, S. P.; Parker, J. E.; Marchal, J.; Potter, J.; Birt, A.; Yuan, F.; Fearn, R. D.; Lennie, A. R.; Street, S. R.; Tang, C. C.; *J. Synchrotron Rad.* **2011**, *18*, 637.